

Energy transfer among Nd^{3+} ions in garnet crystals

Larry D. Merkle and Richard C. Powell

Department of Physics, Oklahoma State University, Stillwater, Oklahoma 74074

(Received 30 October 1978)

Laser-excited, time-resolved site-selection spectroscopy techniques were used to investigate energy transfer between Nd^{3+} ions in $\text{Y}_3\text{Al}_5\text{O}_{12}$ and $\text{Y}_3\text{Ga}_5\text{O}_{12}$ crystals. The results are consistent with a multistep diffusion type of energy transfer with the mechanisms for diffusion and trapping both involving resonant two-phonon-assisted processes.

I. INTRODUCTION

Although $\text{Y}_3\text{Al}_5\text{O}_{12}:\text{Nd}^{3+}$ is one of the most important and most studied crystalline laser materials,¹ there are still some important physical properties of this system which are not well characterized and understood. Energy transfer between neodymium ions is one example of a physical process which has not been thoroughly investigated in this host. We report here the results of an investigation of energy transfer among Nd^{3+} ions in both $\text{Y}_3\text{Al}_5\text{O}_{12}$ and $\text{Y}_3\text{Ga}_5\text{O}_{12}$ crystals. The technique of laser-excited, time-resolved site-selection spectroscopy was employed. The time dependence and temperature dependence of the energy transfer was found to be consistent with two-phonon-assisted migration and trapping processes.

The study of energy transfer between ions in solids has received renewed interest during the past few years because of the ability to use pulsed laser excitation.² The fast pulse capabilities allow time-resolved spectroscopy techniques to be used to characterize the time evolution of the energy transfer whereas the high-resolution capabilities allow the probing of the effects of the inhomogeneities in the system. Studies of the latter type can be divided into two categories. The first includes the ultrahigh resolution investigations utilizing the fluorescence line narrowing of an inhomogeneously broadened transition.³ The second involves systems whose inhomogeneities give rise to significantly different crystal-field sites for the active ions thus allowing the transitions from ions in nonequivalent crystal-field sites to be distinctly resolvable in the spectrum.⁴ These new experimental techniques have resulted in the requirement for new theoretical models for interpreting the data which account for the effects of both spatial and spectral randomness on the characteristics of energy transfer.^{5,6} So far, these investigations have been applied to only a very few cases and continued experimental and theoretical efforts are both still necessary.

The motivation for the work described here was to further our knowledge of the effects of different microscopic environments on the properties of Nd^{3+}

ions and the transfer of energy between Nd^{3+} ions in garnet crystals. Obtaining this type of information on Nd^{3+} -doped garnet materials is of special interest because of the relevance it has to the laser performance of these materials.¹ It was also hoped that our general understanding of the physics of energy transfer between ions in solids could be enhanced by this work and especially that the experimental information obtained by new laser spectroscopy techniques could be used to check the validity of some of the proposed theories of energy transfer. Again the Nd^{3+} -garnet system was thought to be a good choice for this type of fundamental study since so much previous work has been done in establishing the spectral properties of these materials such as transition-matrix elements and branching ratios. The results of this investigation indicate that the characteristics of energy transfer in $\text{YAIG}:\text{Nd}$ crystals are quite different than previously thought.¹ A combination of proposed theories of migration kinetics and phonon-assisted ion-ion interaction is shown to adequately explain the major portion of the results. However, as has generally been the case when the microscopic details of a complex system are probed, the results are quite complicated and some of them are not completely understood. We also point out where further theoretical development is necessary to provide a more exact description of the real physical situation being investigated.

II. THEORETICAL BACKGROUND

The theoretical approach generally used in recent investigations of energy transfer between rare-earth ions in solids^{7,8} was developed by Yokota and Tanimoto⁹ and includes terms for both the migration of energy among sensitizer ions as well as the direct transfer of energy from an excited sensitizer to an unexcited activator ion by electric dipole-dipole interaction. In this treatment the rate equation for the

concentration of excited sensitizers n_s is

$$\frac{\partial n_s}{\partial t} = -\beta_s n_s + D \nabla^2 n_s - \sum_i W_{sa}(R_i) n_s, \quad (1)$$

where β_s is the intrinsic decay rate of the sensitizer, D is the diffusion coefficient for the sensitizer excitation, R_i is the separation between a given sensitizer-activator pair, and $W_{sa}(R_i)$ represents the strength of the energy-transfer interaction which is discussed below. To obtain the expression for the time dependence of the concentration of excited sensitizers, Eq. (1) must be integrated over time and averaged over the spatial distribution of activators. This is a difficult procedure and was achieved by Yokota and Tanimoto⁹ by assuming a uniform distribution of activators, using an operator expansion for the integrand, and dropping terms in $(Dt^{2/3} W_{sa}^{-1/3} R_{sa}^{-2})^n$ for $n > 3$. Here R_{sa} is the average closest sensitizer-activator separation. Then by use of the Padé approximate technique the solution of Eq. (1) is simplified to

$$n_s(t) = n_s(0) \exp \left[-\beta_s t - \frac{4}{3} \pi^{3/2} C_a W_{sa}^{1/2} R_{sa}^3 t^{1/2} \right. \\ \left. \times \left(\frac{1 + 10.87x + 15.50x^2}{1 + 8.743x} \right)^{3/4} \right], \quad (2)$$

where $x = Dt^{2/3} W_{sa}^{-1/3} R_{sa}^{-2}$ and C_a is the concentration of activator ions. At short times after pulsed excitation the electric dipole-dipole interaction between sensitizers and activators dominates the energy transfer and Eq. (2) reduces to the standard time-dependent expression for the energy-transfer rate in the absence of diffusion.¹⁰⁻¹² At long times after the excitation pulse the diffusion-limited situation is reached in which the time-independent energy-transfer rate can be expressed as

$$\omega_s = 4\pi DC_a \rho, \quad (3)$$

where

$$\rho = 0.676 W_{sa}^{1/4} R_{sa}^{3/2} D^{-1/4} \quad (4)$$

is the trapping radius. Both of these two limiting cases have been observed in studies of energy transfer between rare-earth ions in solids.^{13,14} For the results obtained in this work the fluorescence decays are found to be exponential and the data are consistent with a time-independent energy-transfer rate indicating that the diffusion-limited situation is applicable.

It should be mentioned that there are several other approaches to the treatment of energy transfer involving both diffusion among sensitizers as well as direct interaction with activators. The treatment of Kurskii and Selivanenko¹⁵ has been shown to be equivalent to that of Yokota and Tanimoto⁹ when used to fit the same experimental data. The results of Burshtein *et al.*,¹⁶ reduce to the expressions of

Yokota and Tanimoto in the limit of weak diffusion while in the limit of strong diffusion their expressions are equivalent to those of the theory developed by Soos and Powell¹⁷ which is applicable to the physical situation of large trapping regions surrounding activators. Thus, the Yokota-Tanimoto formalism outlined above appears to provide the best available description to the physical situation of interest in this work.

Next, it is necessary to obtain the theoretical expression for the diffusion coefficient in Eq. (3) in terms of the sensitizer ion-ion interaction rate. This is a well-known mathematical problem which is generally treated by setting up the problem in a random-walk formalism and showing the equivalence between the random-walk picture and diffusion in the limit of many steps in the random walk.¹⁸ In this approach the diffusion coefficient is described in terms of the average random-walk hopping time t_h by the expression $D = R_{sa}^2/6t_h$. The hopping time is then expressed in terms of the physical interaction causing the hop to occur. Trlifaj¹⁹ has applied this approach to the specific problem of excitons migrating via electric dipole-dipole interaction and finds the resulting expression for the diffusion coefficient to be

$$D = 3.4 C_s^{4/3} R_{ss}^6 W_{ss}, \quad (5)$$

where C_s is the sensitizer concentration, R_{ss} is the sensitizer-sensitizer separation, and W_{ss} is the interaction strength between two sensitizers. It should be noted that this expression is exactly true only for the case of a random walk on a simple cubic lattice with each step having the same hopping time. For the physical situation of interest here the migration occurs on a lattice of randomly distributed sites resulting in the possibility of significantly different hopping times for different steps. In order to apply this result to the case of interest, it is necessary to use the average Nd-ion separation for R_{ss} and the average interaction strength at this separation. Although it has been shown²⁰ that the formal random-walk results remain unchanged when a small hopping-time dispersion is introduced and accounted for by using the average value of t_h , it is not clear that a large dispersion in hopping times can be legitimately handled in the same simple way. We are currently investigating the effects of treating broad distributions of hopping times in this formalism using Monte Carlo numerical procedures.²¹ However, at the present time, this is the only method we have of treating the problem, and thus, we will follow the usual practice of utilizing Eq. (5) with average values for the parameters.

Finally, it is necessary to decide on the appropriate expression to use for the ion-ion interaction rates. This depends on the mechanism of the interaction (exchange, electric dipole-dipole, etc.) and on wheth-

er the transfer is resonant or phonon assisted. These questions cannot be answered until the experimental results are analyzed but it is possible to speculate about the various possibilities. First, the optical transitions of trivalent neodymium ions in solids are generally thought to occur by forced electric dipole transitions,⁸ and, therefore, the energy transfer between two Nd³⁺ ions is usually considered to take place through forced electric dipole-dipole interaction.²² Second, it has been suggested that the small energy mismatch in the transitions of two similar ions must be made up by two-phonon processes instead of a one-phonon process since the density of states of very low-energy phonons is quite small and a single long-wavelength phonon may modulate the environments of two closely spaced impurity ions in the same way instead of providing the necessary modulation of one ion with respect to the other.⁵ There are many different combinations of possible two-phonon processes resulting in a variety of different possible temperature dependences for the energy-transfer rate such as T^3 , T^7 , and $\exp(-\delta/k_B T)$, where δ is the energy between one of the states involved in the energy-transfer transition and a real intermediate state reached by the phonons involved.

The procedure used in analyzing the data in this work was to first determine from the time dependence of the energy-transfer rate the nature of the interaction mechanism and whether or not we are dealing with a diffusion-limited case. Then from the temperature dependence the nature of the phonon assisting processes was determined. Finally, the magnitude of the energy-transfer rate determined from fitting the data was compared to that predicted by the expression

$$\omega_s = 21.2 C_a C_s R_{Nd}^6 W_{ss}(T)^{3/4} W_{sa}(T)^{1/4} \quad (6)$$

derived above using known parameters for Nd³⁺ ions in garnet crystal hosts and the appropriate expression for the phonon-assisted interaction rate. Here both R_{ss} and R_{sa} have been set equal to the average Nd³⁺-ion separation R_{Nd} . The details of this procedure are described further in Sec. V.

III. EXPERIMENTAL

The samples investigated were good single crystals of Y₃Al₅O₁₂ containing 0.85% ($1.17 \times 10^{20} \text{ cm}^{-3}$) neodymium and Y₃Ga₅O₁₂ containing 0.25% ($3.23 \times 10^{19} \text{ cm}^{-3}$) neodymium. These were mounted in a cryogenic refrigerator capable of varying temperature between about 7 and 300 K. Broadband excitation was provided by a 150-W xenon lamp while a nitrogen-laser-pumped tunable dye laser was used for selective excitation. With rhodamine 6G dye, the laser provided pulses less than 10 nsec in duration and less than 0.4 Å in half-width. The peak power of

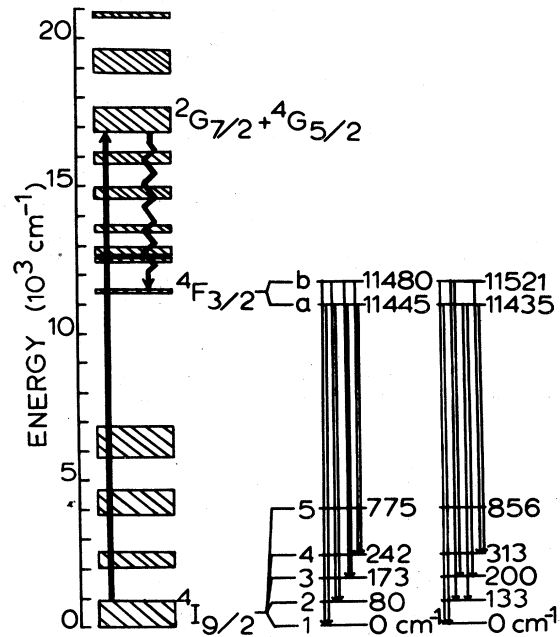


FIG. 1. Energy levels of Nd³⁺ ions in Y₃Ga₅O₁₂, and Y₃Al₅O₁₂ crystals.

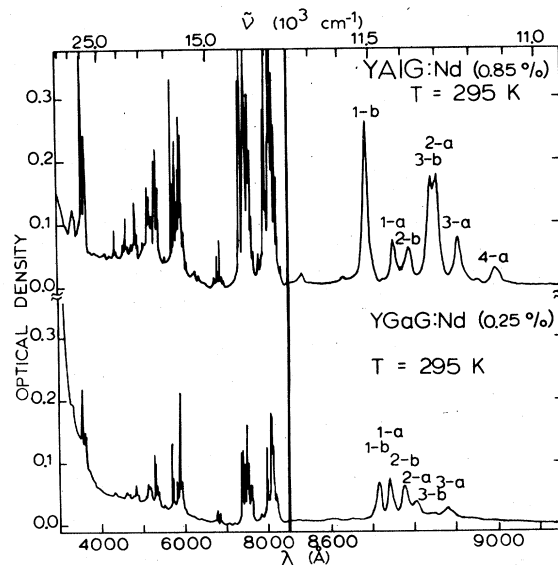


FIG. 2. Room-temperature absorption spectra of Y₃Ga₅O₁₂:Nd³⁺ (3.0 mm thick) and Y₃Al₅O₁₂:Nd³⁺ (2.9 mm thick).

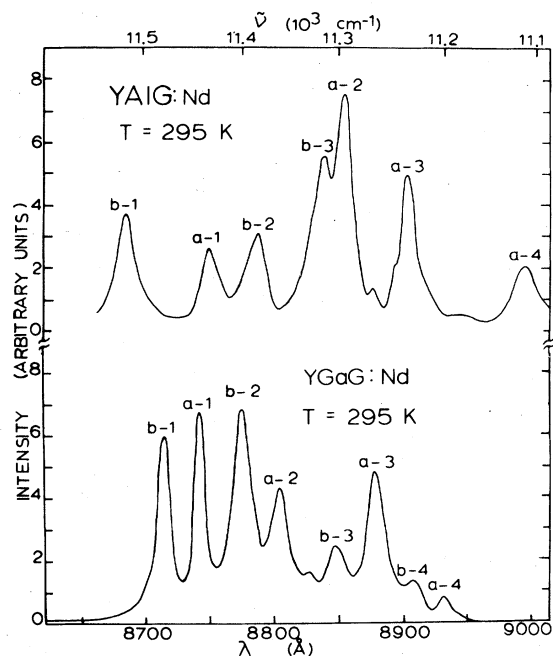


FIG. 3. Room-temperature fluorescence spectra of the ${}^4F_{3/2}$ - ${}^4I_{9/2}$ transitions under broadband excitation. (See Fig. 1 for the transition designations of the lines.)

the pulses was approximately 200 kW at a 30 Hz repetition rate. The sample fluorescence was analyzed by a 1-m spectrometer capable of a resolution in first order of 0.16 Å. The signal was detected by a cooled RCA C31034 photomultiplier tube, averaged by a boxcar integrator triggered by the laser, and displayed on a strip-chart recorder. The time resolution used was about 0.1 μsec.

Figure 1 shows the energy levels relevant to this investigation of Nd^{3+} in the two types of garnet host crystals. Our results are quite similar to those published previously.²³⁻²⁵ With the experimental equipment described above, the ions are pumped in the various components of the ${}^2G_{7/2}$ and ${}^4G_{5/2}$ states and fluorescence occurs after radiationless relaxation to the ${}^4F_{3/2}$ levels. We monitored the fluorescence transitions from this metastable state to the four lowest components of the ${}^4I_{9/2}$ ground-state manifold.

Figure 2 shows the absorption spectra in the region of pumping and fluorescence at room temperature while Fig. 3 shows the fluorescence spectra at room temperature under broadband excitation. The differences in relative peak intensities for similar lines show the differences in oscillator strength and branching ratios for the Nd^{3+} transitions in the two different hosts.

Figures 4 and 5 show the fluorescence spectra for the two samples at low temperatures under selective excitation at short times after the laser pulse. The

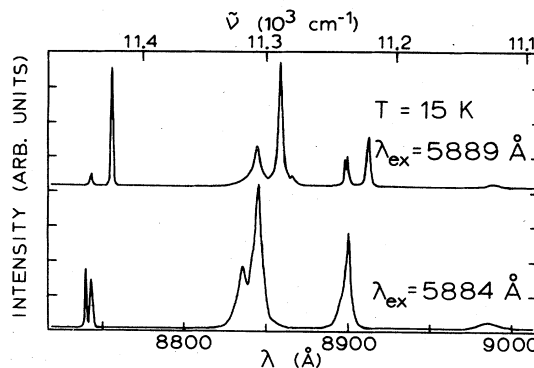


FIG. 4. Fluorescence spectra of $\text{Y}_3\text{Al}_5\text{O}_{12}:\text{Nd}^{3+}$ at low temperatures for two different narrow line laser-excitation wavelengths.

structure in the spectra near each major line is indicative of the variation of transition energies for ions in nonequivalent crystal-field sites. The variation of this structure with pumping wavelength indicates that ions in specific types of crystal-field sites are being selectively excited. For each sample, comparison of the intensities of the same transitions in absorption and emission spectra show that the branching ratios and oscillator strengths are quite different for ions in different crystal-field sites.

The fluorescence lifetimes were measured to be about 200 μsec for the $\text{Y}_3\text{Al}_5\text{O}_{12}$ host and 250 μsec for the $\text{Y}_3\text{Ga}_5\text{O}_{12}$ host. These are essentially temperature independent for the range investigated. Also they were found to be the same within experimental error for ions in all of the major sites which could be selectively excited in both host crystals.

The relative integrated fluorescence intensities of transitions from ions in different crystal-field sites change as a function of time after the laser pulse.

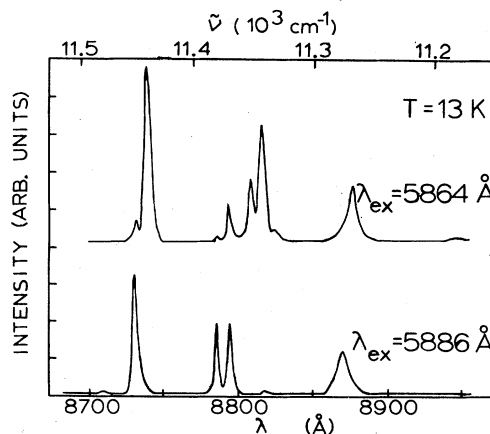


FIG. 5. Fluorescence spectra of $\text{Y}_3\text{Ga}_5\text{O}_{12}:\text{Nd}^{3+}$ at low temperatures for two different narrow line laser-excitation wavelengths.

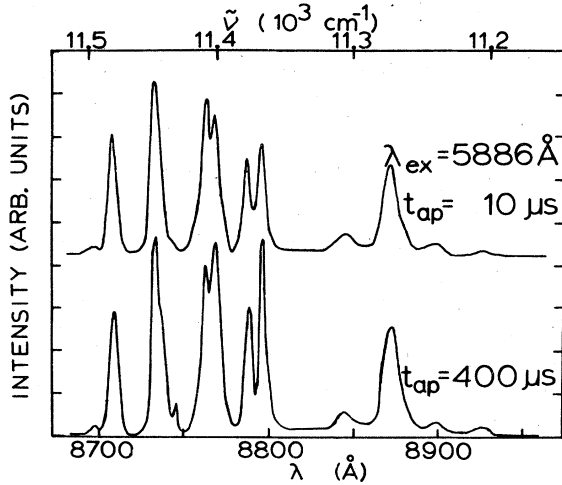


FIG. 6. Fluorescence spectra of $Y_3Ga_5O_{12}:Nd^{3+}$ at 100 K for two different times after the laser pulse (t_{ap}).

Since the fluorescence lifetimes are found to be essentially the same for ions in all major types of sites in the same host, this time dependence can be attributed to energy transfer among ions in different types of sites. Figure 6 shows an example of the fluorescence spectrum of Nd^{3+} in the yttrium gallium garnet sample at 100 K at two different times after the laser pulse. Figure 7 shows the time dependence

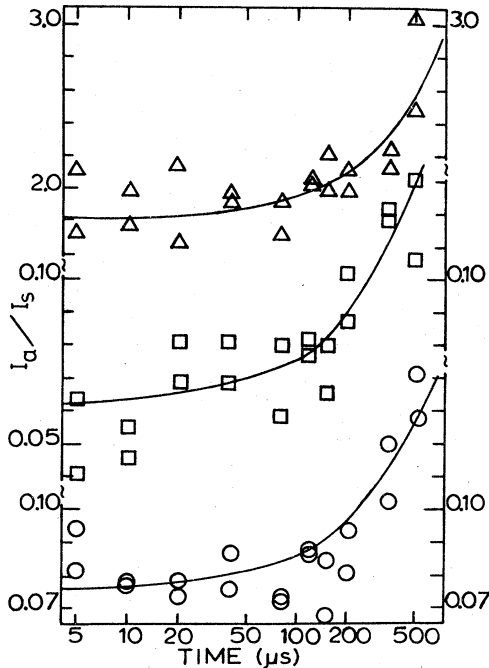


FIG. 7. Ratios of the integrated fluorescence intensities of transitions from Nd^{3+} ions in different crystal-field sites in $Y_3Ga_5O_{12}$ as a function of time after the laser pulse at 100 K. Δ — $I_{8796} \text{ \AA}/I_{8788} \text{ \AA}$; \square — $I_{8744} \text{ \AA}/I_{8732} \text{ \AA}$; \circ — $I_{8697} \text{ \AA}/I_{8708} \text{ \AA}$. (See text for explanation of theoretical lines.)

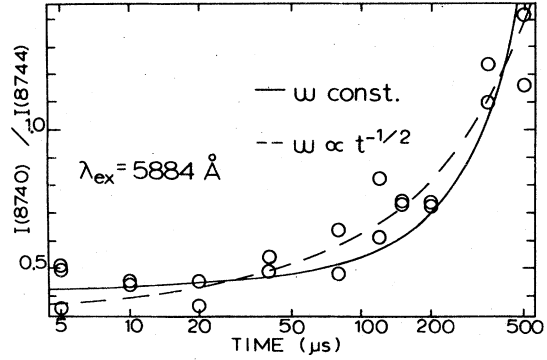


FIG. 8. Time dependence of the integrated fluorescence intensity ratios of lines from Nd^{3+} ions in different crystal-field sites in $Y_3Al_5O_{12}$ at 15 K. (See text for explanation of theoretical lines.)

ences of the relative integrated fluorescence intensity ratios of three sets of lines in this spectrum. Similar results are observed for the yttrium aluminum garnet host. The time dependences are much stronger at high temperatures than at low temperatures. However, above 200 K no site selection can be detected probably due to the phonon broadening of the terminal state of the pumping transitions. Below about 25 K the time dependence of the relative intensities ratios of ions in different types of sites is essentially negligible in the $Y_3Ga_5O_{12}:Nd^{3+}$ sample. At these lowest temperatures in the $Y_3Al_5O_{12}:Nd^{3+}$ sample the relative intensity ratios vary with time in the opposite direction as that observed at high temperatures. An example of this time dependence is shown in Fig. 8.

IV. ANALYSIS

The time-resolved site-selection results on energy transfer between ions in different types of crystal-field sites described above can be analyzed, using a simple two site model with the rate parameters shown in Fig. 9. The rate equations for the populations of the excited states of the two sites can be written

$$\frac{dn_s}{dt} = W_s - \beta n_s - \omega_s n_s + \omega_a n_a, \quad (7a)$$

$$\frac{dn_a}{dt} = W_a - \beta n_a + \omega_s n_s - \omega_a n_a, \quad (7b)$$

where W_s and W_a are the pumping rates, β is the intrinsic fluorescence decay rate, ω_s and ω_a are the energy transfer and back transfer rates between the sensitizer and activator sites and ΔE is the energy mismatch between the excited levels of the ions in the two sites. In order to solve these equations a

specific mechanism must be assumed for the energy-transfer process to determine the time dependence of the transfer rate.

First let us consider the data obtained on the $\text{Y}_3\text{Ga}_5\text{O}_{12}:\text{Nd}^{3+}$ sample. The energy transfer was characterized for an excitation wavelength of 5886 Å. At low temperature it was difficult to detect any time dependence of the relative fluorescence intensities, and it is concluded that very little energy transfer is taking place. At 100 K a distinct time dependence is

$$\frac{I_a}{I_s} = K \left(\frac{(\omega_s/\omega_a)(1 + n_{a0}/n_{s0}) - (\omega_s/\omega_a - n_{a0}/n_{s0}) \exp[-(\omega_s + \omega_a)t]}{(1 + n_{a0}/n_{s0}) + (\omega_s/\omega_a - n_{a0}/n_{s0}) \exp[-(\omega_s + \omega_a)t]} \right), \quad (8)$$

where K represents the ratio of the oscillator strengths and branching ratios for the transitions of the ions in the different crystal-field sites. The average value of the energy-transfer rate needed to give the solid line fits to the data for the three sets of transitions is listed in Table I. The best fits were found with $\omega_a = 0 \text{ sec}^{-1}$.

The data for the $\text{Y}_3\text{Al}_5\text{O}_{12}:\text{Nd}^{3+}$ are more difficult to interpret since the transfer proceeds in one direction at 15 K and in the opposite direction at higher temperatures. The low-temperature data in Fig. 8 can be fit by either Eq. (8) or a similar equation with the transfer rate replaced by $\omega \rightarrow \omega t^{-1/2}$ to show an explicit time dependence. As the solid and dashed lines in the figure indicate, the $t^{-1/2}$ time dependence for the transfer rate gives a somewhat better fit to the data than the constant rate but the latter cannot be ruled out by this analysis. The fitting parameters are listed in Table I.

The temperature dependence of the energy-transfer rate can be determined from Eq. (8) and measure-

ments at very short and long times after the laser pulse. The results for the $\text{Y}_3\text{Ga}_5\text{O}_{12}:\text{Nd}^{3+}$ are shown in Fig. 10. Above about 30 K the transfer rate is found to increase exponentially with an activation energy of about 83 cm^{-1} . In analyzing these data the factor K accounting for differences in branching ratios is taken to be independent of temperature. A similar analysis was made of the $\text{Y}_3\text{Al}_5\text{O}_{12}:\text{Nd}^{3+}$ data and an exponential temperature dependence was again found for the transfer rate as shown in Fig. 11. In this case the weak energy transfer observed at low temperatures was treated as a temperature-independent back transfer process at high temperatures. The activation energy is about 140 cm^{-1} .

V. INTERPRETATION

Since the observed energy-transfer rate is found to be independent of time, energy migration among sensitizer ions may be treated in the diffusion limited regime and the use of Eq. (6) is justified. The temperature dependence appears to be the key in understanding the energy transfer in this case. For an exciton hopping type of energy-transfer phonons can effect the hopping rate in two different ways.²³ The first is enhanced diffusion when new transitions are thermally activated.¹³ The activation energies for both samples are consistent with the splitting between the ground state and the first excited states of the $^4I_{9/2}$ manifold. This explanation might be reasonable for the $\text{Y}_3\text{Al}_5\text{O}_{12}:\text{Nd}^{3+}$ sample for which the $a-2$ transition is much stronger than the $a-1$ transition. However, this is not true for the $\text{Y}_3\text{Ga}_5\text{O}_{12}:\text{Nd}^{3+}$ sample and a consistent explanation for both samples should be expected. The second possible effect is a thermal activation required for either the hopping or trapping steps. The only way we were able to obtain a consistent fit to all of the data was by assuming that both the migration and trapping steps are thermally activated by one of the two-phonon-assisted energy-transfer processes suggested by Holstein *et al.*⁵ The mechanism providing the good fits to the data is one

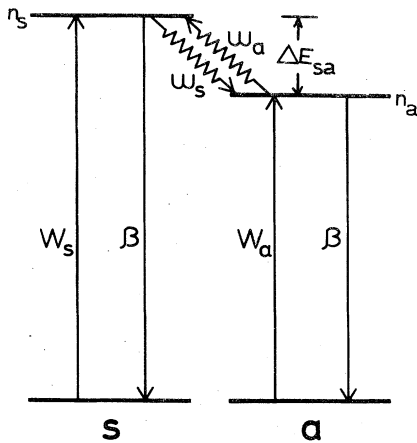
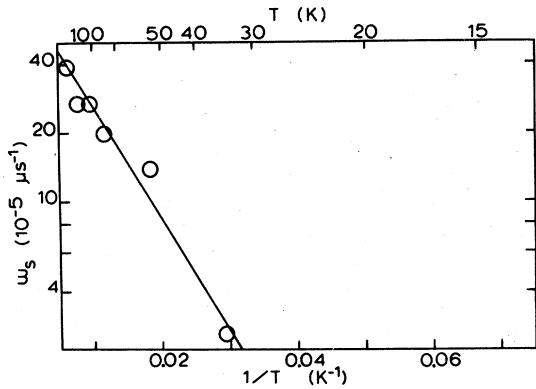
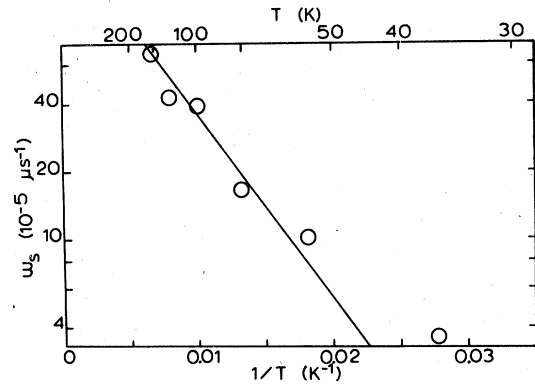


FIG. 9. Energy level and transition rate model used for explaining energy transfer between Nd^{3+} ions in different crystal-field sites. (See text for explanation of symbols.)

TABLE I. Energy-transfer parameters.

	Y ₃ Al ₅ O ₁₂ :Nd ³⁺ (1.18 × 10 ²⁰ cm ⁻³)	Y ₃ Ga ₅ O ₁₂ :Nd ³⁺ (3.24 × 10 ¹⁹ cm ⁻³)
Spectral parameters		
C_s (cm ⁻³)	1.1 × 10 ²⁰	2.7 × 10 ¹⁹
C_a (cm ⁻³)	8.4 × 10 ¹⁸	5.4 × 10 ¹⁸
$\Delta\bar{\nu}_{ss}^{\text{inhomo}}$ (cm ⁻¹)	~1.5	~1.5
ΔE_{sa} (cm ⁻¹)	5.2	6.6
ΔE_{12} (cm ⁻¹)	133	80
Γ (cm ⁻¹)	~7	~5
τ_s^0 (sec ⁻¹)	2.0 × 10 ⁻⁴	2.5 × 10 ⁻⁴
Estimated parameters		
$J_{a1}^2 R_{Nd}^6$ (cm ⁴)	0.6 × 10 ⁻⁵⁰	3.5 × 10 ⁻⁵⁰
$J_{a2}^2 R_{Nd}^6$ (cm ⁴)	12.0 × 10 ⁻⁵⁰	3.9 × 10 ⁻⁵⁰
Fitting parameters		
ω_s (sec ⁻¹) ^a	3.9 × 10 ²	1.4 × 10 ²
ω_a (sec ⁻¹)	2.5 × 10 ³	0
δ (cm ⁻¹)	140	83
ΔE_{ss} (cm ⁻¹)	0.29	0.35
Model parameters		
D_0 (cm ² sec ⁻¹)	6.7 × 10 ⁻¹⁰	2.9 × 10 ⁻¹⁰
D (cm ² sec ⁻¹) ^b	3.5 × 10 ⁻¹⁰	2.0 × 10 ⁻¹⁰
l (cm) ^b	6.5 × 10 ⁻⁷	5.5 × 10 ⁻⁷

^aT = 100 K.^bT = 295 K.FIG. 10. Temperature dependence of the energy-transfer rate between Nd³⁺ ions in nonequivalent crystal-field sites in Y₃Ga₅O₁₂. (See text for explanation of theoretical line.)FIG. 11. Temperature dependence of the energy-transfer rate between Nd³⁺ ions in nonequivalent crystal-field sites in Y₃Al₅O₁₂. (See text for explanation of theoretical line.)

in which the two phonons are in resonance with a nearby real electronic state. The transfer rate between ions i and j for this mechanism is

$$W_{ij} = \left(J_1^2 + J_2^2 \frac{2(\Delta E_{ij})^2}{(\Delta E_{ij})^2 + 8\Gamma^2} \right) \left(\frac{2\Gamma}{\hbar(\Delta E_{ij})^2} \right) \times \left[1 + \exp\left(\frac{\Delta E_{ij}}{kT}\right) \right] \exp\left(\frac{-\delta}{kT}\right), \quad (9)$$

where J_1 and J_2 are the matrix elements for transfer involving the initial excited state and the ground state and for transfer involving the intermediate state reached by the phonons, respectively. ΔE_{ij} is the energy mismatch between the transitions of the two ions involved in the transfer process, δ is the energy of the resonant phonons, and Γ is the width of the intermediate state reached by the phonons. For the Nd-Nd energy transfer considered here the exponential factor involving δ dominates the temperature dependence and is consistent with the splitting of the lowest two components of the $^4I_{9/2}$ ground-state manifold.

If both sensitizer-sensitizer and sensitizer-activator interactions are described by the expression for two-phonon-assisted energy transfer given in Eq. (9), the measured transfer rate is expressed as

$$\omega_s = 71.6 C_a C_s R_{\text{Nd}}^6 \left(\frac{\Gamma}{\hbar} \right) (1 + e^{\Delta E_{sa}/kT})^{1/4} \times \left(\frac{J_1^2}{\Delta E_{ss}^2} + \frac{J_2^2}{4\Gamma^2} \right)^{3/4} \times \left(\frac{J_1^2}{\Delta E_{sa}^2} + \frac{2J_2^2}{\Delta E_{sa}^2 + 8\Gamma^2} \right)^{1/4} e^{-\delta/kT}, \quad (10)$$

where it has been assumed that ΔE_{ss} is small compared to Γ and kT .

The solid lines in Figs. 10 and 11 represent the best fits to the data given by Eq. (10) with the values for δ being the differences between the ground and first excited state in each sample. To obtain these fits to the data it was necessary to estimate the concentrations of sensitizer and activator ions, the strengths of the matrix elements, the widths of the intermediate states reached by the phonons, the sensitizer-activator energy mismatches, and an average value for the energy mismatch between sensitizer ions. Although variations of oscillator strengths between ions in different sites complicate the matter, high-resolution absorption data at low temperature can be used to estimate the concentrations of ions in different sites from relative line strengths. For the types of sites investigated in $\text{Y}_3\text{Al}_5\text{O}_{12}:\text{Nd}^{3+}$ the concentrations are $C_s = 1.1 \times 10^{20}$ and $C_a = 8.4 \times 10^{18} \text{ cm}^{-3}$ while for the $\text{Y}_3\text{Ga}_5\text{O}_{12}:\text{Nd}^{3+}$ sample they are $C_s = 2.7 \times 10^{19}$ and $C_a = 5.4 \times 10^{18} \text{ cm}^{-3}$.

Kushida²⁴ has modified the general electric dipole-dipole energy-transfer expressions of Förster¹⁰ and Dexter¹¹ to apply specifically to rare-earth ions. The squared matrix elements can be estimated from his expression

$$J_{fi}^2 = \frac{(\frac{2}{3})(e^2/R^3)^2}{(2J_s+1)(2J_a+1)} \times \left(\sum_k \Omega_{sk} |\langle J_s || U^{(k)} || J_s' \rangle|^2 \right) \times \left(\sum_k \Omega_{ak} |\langle J_a || U^{(k)} || J_a' \rangle|^2 \right), \quad (11)$$

where f and i indicate the final and initial states of the systems, R is the separation between the two ions, and the Ω are the Judd-Ofelt parameters. The latter have been determined by Krupke²⁵ and for the $^4F_{3/2}-^4I_{9/2}$ transitions the expression for the squared matrix element becomes

$$J_{fi}^2 = (1.39 \times 10^{-23}) \frac{ch^2\lambda^2}{(n^2+2)^4\pi^7 R^6} (\text{erg}^2), \quad (12)$$

where n is the refractive index of the crystal at the wavelength of the fluorescence λ . A factor for the branching ratio must be included to determine the squared matrix elements for specific transitions between individual crystal-field levels within the ground and excited multiplets. For the two transitions of interest in expression (10) the squared matrix elements have the values

$$J_{a1}^2 = 0.6 \times 10^{-50} R_{\text{Nd}}^{-6} \text{ cm}^4, \\ J_{a2}^2 = 12.0 \times 10^{-50} R_{\text{Nd}}^{-6} \text{ cm}^4,$$

for $\text{Y}_3\text{Al}_5\text{O}_{12}:\text{Nd}^{3+}$; (13)

$$J_{a1}^2 = 3.5 \times 10^{-50} R_{\text{Nd}}^{-6} \text{ cm}^4, \\ J_{a2}^2 = 3.9 \times 10^{-50} R_{\text{Nd}}^{-6} \text{ cm}^4,$$

for $\text{Y}_3\text{Ga}_5\text{O}_{12}:\text{Nd}^{3+}$.

The level width of the intermediate state can be taken from measured spectral data to be about 7 cm^{-1} for the aluminum garnet host and about 5 cm^{-1} for the gallium garnet. Also, the sensitizer-activator energy mismatches are measured to be about 5.2 cm^{-1} for the aluminum garnet sample and 6.6 cm^{-1} for the gallium garnet.

The various estimated values of the parameters given in the preceding three paragraphs can be substituted into Eq. (10). The remaining unknown parameter in the equation is the average transition energy mismatch between two sensitizer ions. An upper bound on ΔE_{ss} is the inhomogeneous linewidth for

the sensitizer transitions $\Delta\tilde{\nu}_{ss}^{\text{inhomo}}$ which is measured to be of the order of one and a half wave numbers. The best fits to the data using Eq. (10) are shown as solid lines in Figs. 10 and 11. They required values of ΔE_{ss} of about one-third of a wave number which is somewhat less than the inhomogeneous linewidth as expected.

With the estimated parameters and those obtained from fitting the data, it is now possible to obtain a value for the diffusion coefficient from Eqs. (5) and (9) with the temperature dependence expressed explicitly as

$$D = D_0 e^{-8/kT} \quad (14)$$

The values of D_0 and D at room temperature are listed in Table I. The diffusion length l can be estimated from the expression²³

$$l = (6D\tau_s^0)^{1/2} \quad (15)$$

Again the room-temperature values of this parameter are listed in Table I. Note that the extrapolation of these parameters to room temperature may not give exact values but it provides useful estimates for comparison to other data obtained at room temperature.

VI. DISCUSSION AND CONCLUSIONS

To summarize, the time-dependent and temperature-dependent data obtained on energy transfer between Nd³⁺ ions in two different garnet host crystals can only be explained by a multistep energy migration process where both the hopping between ions in similar types of sites and the transfer of energy to ions in nonequivalent crystal-field sites take place by a two-phonon-assisted mechanism involving resonant transitions between the ground and first excited states. For both hosts the sites which are selectively excited by the narrow-band laser pulse are the dominant types of sites for Nd³⁺ ions in the lattice whereas there are significantly less Nd³⁺ ions in activator-type sites. The nature of the different types of crystal-field sites is not known but the dominant sensitizer sites may be Nd³⁺ ions in unperturbed Y³⁺ lattice sites whereas the less populous activator sites may be Nd³⁺ ions in sites near to lattice defects or impurities which alter the local crystal-field environment. It is well known that substitutional impurities purposely introduced into the garnet lattice produce a variety of sites with different transition energies for Nd³⁺ ions.^{23,26} It should be noted that time-independent energy-transfer rate could also indicate single-step transfer between sensitizer-activator pairs all at the same fixed distances. This type of distribution is not physically reasonable unless some clustering of Nd³⁺ ions occurs. Clustering, however, would lead to cross-relaxation quenching which is not observed.

The major complication in interpreting the results is the complex nature of the system. The excitation energy is migrating on a lattice of randomly distributed sites with a superimposed random distribution of transition energies. No exact method for treating this problem has been developed, and it may be that numerical techniques are the only possible solution.^{5,6} The theoretical approach used here assumes that the inhomogeneities in the transition energies are more important in determining energy-transfer characteristics than the inhomogeneities in the spatial distribution of ions. Thus, the expressions describing exciton diffusion in Eqs. (3), (5), and (15) are all based on a uniform distribution of ions with the transition energy inhomogeneities accounted for in the expression for microscopic ion-ion interaction rates. This approach appears to give a reasonable explanation of the energy-transfer characteristics in the systems investigated here, but a more exact approach to this problem would certainly be desirable. Also, for the small values of $W_{sa}R_{Nd}^0$ encountered in this case, it may be necessary to include higher-order terms in the expansion used to derive Eq. (2). Thus, the magnitudes of the parameters obtained from this analysis must be considered as only rough estimates.

The nature of the residual energy transfer at very low temperatures in the Y₃Al₅O₁₂:Nd³⁺ sample is still not completely understood especially with respect to the fact that the transfer proceeds in the opposite direction from that observed at higher temperatures. It may be that for some reason the site selection is different at low and high temperatures, but this is not apparent from any spectral observations. Maintaining exactly the same selective excitation at all temperatures is difficult when the pumping is to a higher excited state consisting of numerous, relatively broad levels. Also, it is not understood why the resonant phonon processes in the ground-state manifold dominate the temperature dependence instead of similar processes involving the components of the ⁴F_{3/2} state which have a smaller splitting. However, it is interesting to note that Kushida²⁷ has found that the thermal broadening of these transitions is also attributable to phonon processes in the ground state. Also, migration of energy among Nd³⁺ ions in a glass host has been found to have a thermal activation energy of ~150 cm⁻¹.²⁸

The value of D of the order of 10⁻¹⁰ cm² sec⁻¹ is similar to the values found for energy migration among other rare-earth ions in solids which range from 10⁻⁹ to 10⁻¹⁴ cm² sec⁻¹.²⁹ Although a significant amount of the difference in D_0 for the two samples can be accounted for simply by the difference in sensitizer concentrations, the diffusion coefficient for Nd excitons will be intrinsically larger in the Y₃Al₅O₁₂ host compared to the Y₃Ga₅O₁₂ host due to the increased values of the matrix elements in Eq. (9) which make W_{ss} larger in Eq. (5). Note that in-

creased inhomogeneous broadening will decrease D_0 by decreasing W_{ss} in Eq. (5). There are two previous estimates of the energy diffusion characteristics for the $Y_3Al_5O_{12}:\text{Nd}^{3+}$ system. Danielmeyer, Blatte, and Balmer²⁹ theoretically estimated a diffusion length of about 500 Å from spectral considerations and Danielmeyer³⁰ determined the anomalously large value of $D = 5 \times 10^{-7} \text{ cm}^2 \text{ sec}^{-1}$ for a sample containing only 0.4% Nd^{3+} from analyzing its single-mode laser operation. The time-resolved site-selection technique utilized in the experiments reported here is the most direct way of characterizing the energy migration reported thus far.

In conclusion, laser-excited time-resolved site-selection spectroscopy has been used to characterize the transfer of energy among Nd^{3+} ions in two types of garnet host crystals and the results interpreted in terms of an exciton diffusion and trapping model.

Both the diffusion and trapping mechanisms are consistent with the predictions of one of the new theoretical models for two-phonon-assisted transfer processes. The migration parameters obtained in this way are consistent with those obtained for other similar systems but it is obvious that there is an important need for an exact way to theoretically treat cases of energy migration on a random lattice.

ACKNOWLEDGMENTS

This work was supported by the U. S. Army Research Office. The authors are grateful to R. K. Watts for supplying us with the samples used in this work and determining their neodymium concentrations. We also gratefully acknowledge the help and useful discussions on this work with G. F. Imbusch and B. DiBartolo.

- ¹H. G. Danielmeyer, in *Lasers*, Vol. 4, edited by A. K. Levine and A. J. DeMaria (Dekker, New York, 1976), p. 1.
- ²R. C. Powell, in *Luminescence of Inorganic Solids*, edited by B. DiBartolo (Plenum, New York, 1978), p. 547.
- ³N. Motegi and S. Shionoya, *J. Lumin.* **8**, 1 (1973); R. Flach, D. S. Hamilton, P. S. Selzer, and W. M. Yen, *Phys. Rev. B* **15**, 1248 (1977); P. M. Selzer, D. S. Hamilton, and W. M. Yen, *Phys. Rev. Lett.* **38**, 858 (1977); D. S. Hamilton, P. M. Selzer, and W. M. Yen, *Phys. Rev. B* **16**, 1858 (1977); P. M. Selzer, D. L. Huber, B. B. Barnett, and W. M. Yen, *Phys. Rev. B* **17**, 4979 (1978); R. Flach, D. S. Hamilton, P. S. Selzer, and W. M. Yen, *Phys. Rev. Lett.* **35**, 1034 (1975).
- ⁴C. Hsu and R. C. Powell, *Phys. Rev. Lett.* **35**, 734 (1975); C. Hsu and R. C. Powell, *J. Phys. C* **9**, 2467 (1976); G. E. Venikouas and R. C. Powell, *Phys. Rev. B* **17**, 3456 (1978); L. D. Merkle and R. C. Powell, *J. Chem. Phys.* **67**, 371 (1977); D. R. Tallant and J. C. Wright, *J. Chem. Phys.* **63**, 2074 (1975); M. D. Kurz and J. C. Wright, *J. Lumin.* **15**, 169 (1977).
- ⁵T. Holstein, S. K. Lyo, and R. Orbach, *Phys. Rev. Lett.* **36**, 891 (1976); T. Holstein, S. K. Lyo, and R. Orbach, *Phys. Rev. B* (to be published). A preliminary account of this work was presented at the Colloque International du Centre National de la Recherche Scientifique, 1976 (unpublished).
- ⁶D. L. Huber, D. S. Hamilton, and B. Barnett, *Phys. Rev. B* **16**, 4642 (1977); W. Y. Ching, D. L. Huber, and B. Barnett, *Phys. Rev. B* **17**, 5025 (1978).
- ⁷R. K. Watts, in *Optical Properties of Ions in Solids*, edited by B. DiBartolo (Plenum, New York, 1975).
- ⁸L. A. Riseberg and M. J. Weber, *Prog. in Opt.* **14**, 1 (1975).
- ⁹M. Yokota and O. Tanimoto, *J. Phys. Soc. Jpn.* **22**, 779 (1967).
- ¹⁰T. Förster, *Ann. Phys. (Paris)* **2**, 55 (1948); *Z. Naturforsch.* **49**, 321 (1949).
- ¹¹D. L. Dexter, *J. Chem. Phys.* **21**, 836 (1953).
- ¹²K. B. Eiselenthal and S. Siegel, *J. Chem. Phys.* **41**, 652 (1964).
- ¹³M. J. Weber, *Phys. Rev. B* **4**, 2932 (1971).
- ¹⁴W. B. Gandrud and H. W. Moos, *J. Chem. Phys.* **49**, 2170 (1968).
- ¹⁵Y. A. Kurskii and A. S. Selivanenko, *Opt. Spektrosk.* **8**, 340 (1960).
- ¹⁶A. I. Burshtein, *Sov. Phys. JETP* **35**, 882 (1972).
- ¹⁷Z. G. Soos and R. C. Powell, *Phys. Rev. B* **6**, 4035 (1972).
- ¹⁸S. Chandrasekhar, *Rev. Mod. Phys.* **15**, 1 (1943).
- ¹⁹M. Trlifaj, *Czech. J. Phys.* **5**, 463 (1955); **6**, 533 (1956); **8**, 510 (1958).
- ²⁰E. W. Montroll and G. H. Weiss, *J. Math. Phys.* **6**, 167 (1965).
- ²¹D. D. Smith, R. C. Powell, and A. H. Zewail (unpublished).
- ²²T. Kushida, *J. Phys. Soc. Jpn.* **34**, 1318 (1973); **34**, 1327 (1973); **34**, 1334 (1973).
- ²³R. C. Powell and Z. G. Soos, *J. Lumin.* **11**, 1 (1975).
- ²⁴T. Kushida, *J. Phys. Soc. Jpn.* **34**, 1381 (1973).
- ²⁵W. F. Krupke, *IEEE J. Quantum Electron* **QE-7**, 153 (1971).
- ²⁶L. A. Riseberg and W. C. Holton, *J. Appl. Phys.* **43**, 1876 (1972); L. A. Riseberg, R. M. Brown, and W. C. Holton, *Appl. Phys. Lett.* **23**, 127 (1973); L. A. Riseberg and W. C. Holton, *Opt. Commun.* **2**, 298 (1973).
- ²⁷T. Kushida, *Phys. Rev.* **185**, 500 (1969).
- ²⁸M. V. Artamonova, Ch. M. Briskina, A. I. Burshtein, L. D. Zusman, and A. G. Skleznev, *Sov. Phys. JETP* **35**, 457 (1972).
- ²⁹H. G. Danielmeyer, M. Blatte, and P. Balmer, *Appl. Phys.* **1**, 269 (1973).
- ³⁰H. G. Danielmeyer, *J. Appl. Phys.* **42**, 3125 (1971).